4.4 CORRECTING CMAQ PHOTOLYSIS RATES BASED ON GOES OBSERVED CLOUDS

Arastoo Pour Biazar*, Richard T. McNider
University of Alabama in Huntsville

Shawn J. Roselle
EPA/NERL/AMSD, Research Triangle Park

Ronnie J. Suggs
Earth Science Department, NASA/MSFC

1. INTRODUCTION

A key component of air quality modeling is the correct estimation of photodissociation reaction rates (or photolysis rates). Photolysis rates, the rate at which photochemistry takes place, depend on the intensity of solar radiation in the atmosphere and the molecular properties of the molecule undergoing photodissociation. Therefore, attenuation or enhancement of radiant energy due to atmospheric absorption and scattering is important in determining the photolysis rates. Since clouds can significantly alter the solar radiation in the wavelengths affecting the photolysis rates, they can have considerable impact on the photochemistry.

Air quality models rely on radiative transfer models for the prediction of photolysis rates. There are a suite of radiative transfer models [see Barker et al., 2003] that take extraterrestrial solar flux, optical properties of the atmosphere, and surface albedo as input to describe the propagation of radiation in the atmosphere. Radiative transfer models are widely used for both research and in weather and climate models. Barker et al. compared the performance of 25 radiative transfer models with respect to unresolved clouds. They concluded that most of the models used in their study underestimate atmospheric absorption of solar radiation. Other studies [Collins et al., 2000; Liao et al., 1999; Jacobson, 1998; Dickerson et al., 1997; Castro et al., 1997; Ruggaber et al., 1994; Madronich, 1987] have investigated the effects of changes in atmospheric conditions and surface albedo on the estimates of photolysis rates. Most of these studies conclude that aerosols and clouds play an important role in modifying the photolysis rate either by enhancing it due to light scattering, or by reducing it due to absorption and attenuation.

The Community Multiscale Air Quality modeling system (CMAQ, EPA, 1999) uses a two-step approach for calculating the photolysis rates. This approach is similar to that of the Regional Acid Deposition Model (RADM, Chang et al., 1987) and is a typical method used in most air quality models. First, in a preprocessor, a radiative transfer module (based on Madronich, 1987) is used to compute clear sky photolysis rates for a range of latitudes, altitudes, and zenith angles. Then, within the chemical transport model, the tabular photolysis rates are interpolated for each location and corrected for cloud cover.

There are two major concerns with this approach as far as cloud correction is concerned. First, estimation of cloud transmissivity in models is highly parameterized and therefore introduces a large uncertainty. Second and most important, the cloud information is provided by a mesoscale model, which has difficulty with the spatial and temporal placement of clouds and their vertical extent. The mesoscale model used in the CMAQ modeling system is the Fifth-Generation Penn State/NCAR Mesoscale Model (MM5) [Grell et al., 1994; NCAR, 2003].

Unfortunately, standard weather service observations are not sufficiently dense to be used for cloud specification. However, geostationary satellite data can provide the desirable coverage with sufficient spatial resolution. The Geostationary Operational Environmental Satellite (GOES) has the capability to measure cloud properties such as optical reflectance down to scales of 1-km and cloud top heights to 4-km, and for time scales down to an hour or less.

In this paper, we present the results from incorporating satellite derived transmissivity and cloud top height to provide the cloud properties

* Corresponding author address: Arastoo Pour Biazar, Univ. of Alabama in Huntsville, NSSTC, Huntsville, AL 35805 (biazar@nsstc.uah.edu).

needed in photolysis rate calculations, and use these revised photolysis fields in the CMAQ model. This is a first-order incorporation of cloud effects. GOES visible and IR data collected and processed during the Texas Air Quality Study 2000 (TexAQS2000) period are utilized. The impact of the satellite-based photolysis fields on ozone production versus MM5-derived photolysis fields is examined.

2. Current Method for Cloud Correction in CMAQ

Photolysis rate (s^{-1}) is represented by:

$$J = \int_{\lambda_1}^{\lambda_2} \sigma(\lambda)\varphi(\lambda)F(\lambda)d\lambda \qquad (1)$$

Where $\sigma(\lambda)$ (*m^2/molecule*) is the absorption cross-section for the molecule undergoing photodissociation as a function of wavelength λ (μm); $\varphi(\lambda)$, quantum yield (*molecules/photon*), is the probability that the molecule photodissociates in the direction of the pertinent reaction upon absorbing the radiation of wavelength λ; and $F(\lambda)$ is the actinic flux (*photons/m^2/s/μm*).

By providing the actinic flux for clear sky, photolysis rates (J_{clear}) can be calculated by equation (1). In CMAQ, following Chang et al. (1987) and Madronich (1987), these rates are corrected for cloud cover. Below the cloud, the rate is corrected by:

$$J_{below} = J_{clear}\left[1 + f_c(1.6tr_c\cos(\theta) - 1)\right] \qquad (2)$$

Where f_c is the cloud fraction for a grid cell, tr_c is cloud transmissivity, and θ is the zenith angle. The above formulation leads to a lower value for the photolysis rates below the cloud, where the cloud transmissivity is reduced. Above the cloud, photolysis rate is modified as:

$$J_{above} = J_{clear}\left[1 + f_c\alpha\cos(\theta)(1 - tr_c)\right] \qquad (3)$$

Here α is a reaction dependent coefficient that further modifies above the cloud enhancement (Chang et al., 1987). This is to allow for the photolysis rate enhancement that is resulting from the reflected radiation from the cloud top. Within the cloud, the photolysis rates are obtained by interpolating between cloud base and cloud top values. Therefore, based on the formulation above, the cloud transmittance and cloud fraction are required for calculating cloud correction for photolysis rates. Also, since in-cloud photolysis rates are interpolated, cloud base and top heights must also be known.

In CMAQ, the calculation of cloud transmissivity is highly parameterized. The formulation is based on the parameterization suggested by Stephens (1978). Utilizing MM5 information, the Meteorology-Chemistry Interface Preprocessor (MCIP) recovers cloud thickness (H_c) and liquid water content (w). Liquid water path (g/m^2) is then calculated by:

$$LWP = wH_c \qquad (4)$$

Then the broadband cloud optical depth (τ_c) as a function of liquid water path is calculated as:

$$\tau_c = 10^{.2633+1.7095\ln[\log_{10}(LWP)]} \qquad (5)$$

Finally, assuming a scattering phase-function asymmetry factor of .86, cloud transmissivity is calculated by:

$$tr_c = \frac{5 - e^{-\tau_c}}{4 + 3\tau_c(1 - \beta)} \qquad (6)$$

Where β is the scattering phase-function asymmetry factor. As evident from the above formulation, even if the MM5 cloud prediction was correct, there is a large uncertainty in the above calculation of cloud transmittance due to the assumptions used in the parameterization.

From GOES satellite observations, we are able to recover broadband cloud transmissivity and the cloud top height. Also, since GOES cloud mask algorithm can detect clouds at 4-km resolution, an observed cloud fraction can be calculated for coarser grid cells as the fraction of cloudy pixels within a grid cell. Cloud base height is estimated as the local condensation level (LCL) from the information (temperature and mixing ratio fields) provided by the mesoscale model. In this study we replaced tr_c and f_c in equations (2) and (3) with the satellite inferred quantities to perform the cloud correction.

3. GOES broadband visible transmission and cloud top heights

The Infrared Measurement and Processing Group (hereafter IR Group) at the National Space Science and Technology Center performed the satellite retrievals for this study. Currently, the IR group uses GOES Product Generation System (GPGS) to provide routine real-time retrievals of skin temperature, total precipitable water, cloud top pressure, cloud albedo, surface albedo and surface insolation for the use of meteorological and air quality models [Haines et al., 2003]. As input, GPGS needs a first-guess field for its retrievals and the model grid information if the product is to be used in a grid model. For this

study, the MM5 simulation that was utilized for the CMAQ runs provided the required information to GPGS and the retrievals reflected the MM5 grid cell values.

The algorithm used for the retrieval of albedo and surface insolation is the implementation of Gautier et al. (1980) method complemented by the improvements from Diak and Gautier (1983). The method uses the information from GOES Imager visible channel (.52-.72 μm) at 1-km resolution, and employs a clear and a cloudy atmosphere to explain the observed upwelling radiant energy. The model applies the effects of Rayleigh scattering, ozone absorption, water vapor absorption, cloud absorption, and cloud reflection. The effects of Rayleigh scattering are modeled after Coulson (1959) and Allen (1963) for the GOES visible band (radiant flux as viewed by the satellite) and for the bulk solar flux incident at the surface. Ozone absorption is modeled after Lacis and Hansen (1974). Water vapor absorption is assumed to be negligible in both the surface and cloud albedo calculations (explaining the observed radiance in the GOES visible band), but accounted for when applying the total solar flux in the surface insolation calculation. Water vapor absorption coefficients are obtained from Paltridge (1973), and total column water vapor is assumed to be 25 mm and adjusted for solar zenith angle. Cloud absorption is assumed to be a constant 7% of the incident flux at the top of the cloud [Diak and Gautier, 1983].

The first step in calculating cloud albedo is the retrieval of surface albedo. The surface albedo for the entire domain is calculated by using the clear-sky composite image. For the current study, a 20-day composite centered on the period of the case study was used to generate the clear-sky composite image. The single composite image records the minimum albedo value for each pixel for a given hour. Assuming that for any given hour during the day (for the entire 20 day period) each pixel experiences clear-sky at least once, then the minimum value represents the clear-sky value for that pixel. Since the absorption and scattering processes are estimated, the radiation equation is then solved for the only unknown (i.e., the surface albedo). This formulation also assumes that the visible channel surface albedo does not vary significantly within the time period of composite.

The insolation is calculated as the sum of solar radiation incident at the surface from both direct and diffuse sources and also includes the effect of attenuation by clouds. For the clear-sky case, the incident short-wave radiation at the surface is 1) the incident solar flux that is attenuated by Raleigh scattering, ozone and water vapor absorption, and 2) the surface reflected flux scattered back to the surface by Raleigh scattering. With the surface albedo known and the absorption and scattering processes estimated, the surface insolation is calculated directly.

For the cloudy-sky, the radiance observed by the satellite is assumed to be a function of the incident solar flux undergoing several processes. The satellite observed radiant energy is the sum of atmospheric backscatter, reflection of the incident solar flux from the cloud top, backscatter within the cloud by Rayleigh scattering, and the amount of surface reflection that reaches satellite after attenuation. Since the radiance at the satellite, the surface albedo, and estimates of the scattering and absorption are known, the radiation formulation can then be solved for the cloud albedo. In practice, the algorithm calculates a surface insolation using both the clear-sky and cloudy-sky formulations for a given scene. If the cloudy-sky calculation is greater than or equal to the clear-sky value, then the clear-sky value is used and the scene is assumed clear. This is consistent with the cloud albedo being near zero for clear-sky conditions. For thick clouds, a bulk solar cloud absorption of 7% of the incident flux at the cloud top is assumed [Diak and Gautier, 1983]. Since the effect of cloud albedo dominates the insolation calculation, uncertainties in cloud thickness have shown to produce only small effects on the surface insolation calculation.

Since the sum of cloud albedo (A_c), cloud absorption (a_c), and cloud transmittance is 1, then the broadband cloud transmittance is calculated as:

$$tr_c = 1. - (A_c + a_c) \qquad (7)$$

The other needed vital information for our cloud correction is the cloud top height. A cloud top pressure is assigned to each pixel that is determined to be cloudy in the GOES satellite imagery. GOES 11-μm window channel (of either the Imager or the Sounder) brightness temperature is used for this purpose. The clouds are assumed to be uniform in coverage and height over the GOES pixel. The brightness temperature for each cloudy pixel is referenced to the corresponding thermodynamic profile for the closest model grid. No attempt is made to correct the brightness temperature for the effect of water

vapor above the cloud. The pressure assignment is similar to that used by Fritz and Winston (1962) and applied by Jedlovec et al. (2000). Log-linear interpolation is used between model vertical pressure levels to assign a corresponding pressure for the cloud top temperature.

The approach works well for opaque clouds where the cloud emissivity is close to unity and emission (measured by the satellite) comes primarily from the cloud top. Typical pressure assignment errors are on the order of 25-50 mb (for an 11 µm RMS error of 0.5 K and a 2.0 K forecast error). The effect of water vapor on the window channel brightness temperature could produce about a 25mb bias in the heights. This bias would be greatest for low clouds and would result in clouds having assigned pressures that are too low in magnitude.

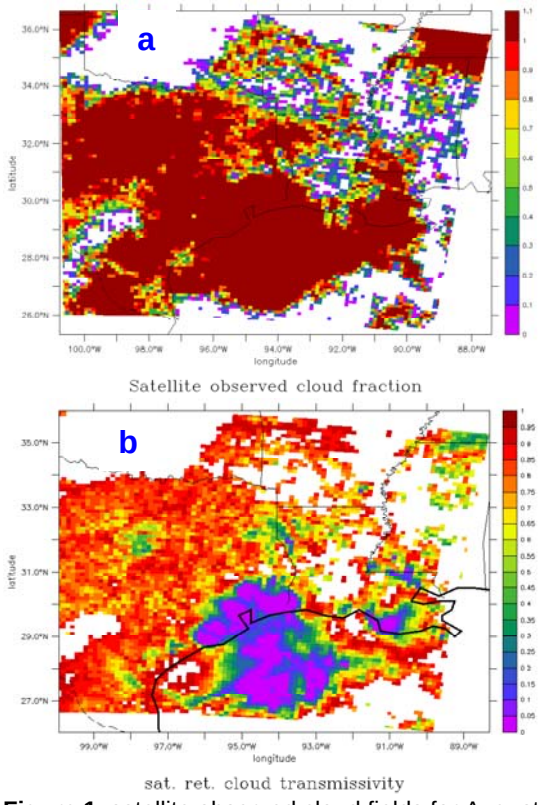

Figure 1. satellite observed cloud fields for August 24, 2000, 21 GMT. a) Cloud fraction; b) cloud transmissivity.

For air quality applications, however, since the focus is on the boundary layer, the error in the cloud top pressure for the opaque clouds does not pose a significant problem. Furthermore, the cloud top height is only used for determination of the atmospheric layer in which photolysis rates are being interpolated, and it does not impact the correction made to the photolysis rates within the boundary layer. In addition, the determination of cloud-top in the model is limited by the vertical resolution of the model, which usually is too coarse in the free-troposphere. For the non-opaque clouds, the cloud transmissivity is large and therefore the modifications to photolysis rates are small and thus the impact of the error in the cloud top height is further reduced. Figures 1a and 1b illustrate a situation on August 24, 2000, where the satellite observation indicates most of the domain is cloudy, yet in fact only the cloud mass over the Galveston Bay area is opaque. For most of the domain, the clouds are almost transparent and the retrieved cloud transmittance is close to 1. For low transparent clouds with unrealistic cloud top pressure, we allow for a thin cloud above the cloud base (only one layer thick).

4. Model Simulations

We implemented the technique described above in the current CMAQ modeling system to perform a set of simulations for 12- and 4-km resolution domains over Texas for the period of August 24 to August 31, 2000. The 12-km domain covers the eastern half of Texas, Louisiana, Mississippi, southern part of Oklahoma and Arkansas, and the southwestern corner of Tennessee. The first set of simulations utilizes CMAQ in its standard configuration, and is used as the control case (hereafter referred to as CMAQ_base) for comparison. The second set of simulations (hereafter referred to as CMAQ_sat) uses the satellite observed cloud information. Both sets of simulations use the same meteorological information from a single MM5 run.

The control MM5 simulation was configured to use FDDA gridded nudging, Dudhia moisture scheme, Grell convective parameterization, Medium Range Forecast (MRF) PBL scheme, RRTM radiation scheme, shallow convection scheme, and 5-layer soil model. Grell cumulus parameterization has proven to be useful for smaller grid sizes (10-30 km). It tends to allow a balance between resolved scale rainfall and convective rainfall.

CMAQ (version 4.3) was configured to use piecewise parabolic method for advection, multiscale horizontal diffusion and eddy vertical diffusion, SMVGEAR chemical solver, 3rd generation aerosol model and 2nd generation aerosol deposition model, RADM cloud model, and SMVGEAR chemical solver. Carbon bond IV

(CB4) chemical mechanism (Gery et al., 1989), including aerosol and aqueous chemistry is utilized to describe atmospheric reactions. The model uses 21 layers, with about 10 layers within the daytime boundary layer. The emissions for this study are based on EPA's 1999 National Emissions Inventory (NEI99, version 2).

5. Results and Discussion

As described in the previous section, the meteorological information to drive CMAQ was obtained from a single MM5 run. This means that there is no change in the dynamic fields for the CMAQ simulations and the differences between CMAQ_base and CMAQ_sat simulations are only due to the impact of observed clouds on the photochemistry. It should be noted, however, that the uncertainty in the standard modeling results could be even greater due to the impact of cloud dynamics on the vertical transport of the pollutants.

For example, on the afternoon of August 24, convective clouds developed over the Galveston Bay and expanded toward north/northwest. This is absent in the MM5 simulation, meaning that the vertical transport of pollutants over the Bay area into these convective cells is missing in our simulations. While our method corrects for the impact of the observed convective clouds on the photochemistry, there are still errors arising from the lack of accurate distribution of pollutants due to errors in the dynamics. Therefore, here we only present model-to-model comparisons to illustrate the first-order photochemical impact of including the observed clouds.

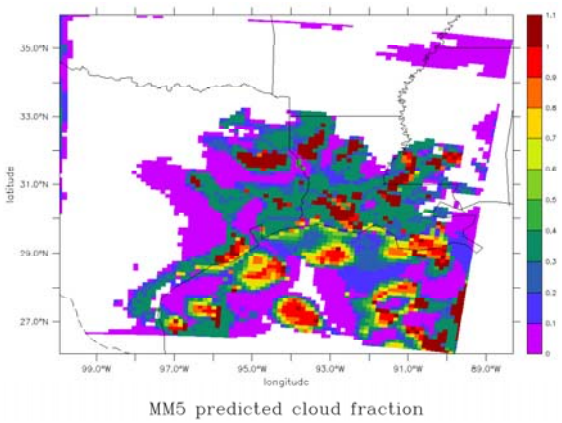

Figure 2. MM5 predicted cloud fraction for August 24, 2000, 21 GMT.

Texas and surrounding areas were extremely dry for the period of our study, and perhaps not the best case to show the benefits of utilizing GOES information. Nevertheless, there was enough cloudiness to show the impact of observed clouds on the photochemical model predictions. Figure 2 shows MM5 predicted clouds for the same time period as in Figure 1 (August 24, 2000, 21 GMT). In comparison to Figure 1, the disagreement between MM5 predicted cloud fields and GOES observations are realized. In the case of August 24, 2000, MM5 predicts clouds to the south/southeast of the domain with most of it being subgrid scale. Only few small areas of grid scale clouds over land are predicted. In contrast, satellite observations indicate large area of cloudiness extending from south/southeast to the northwest part of the domain. Satellite observation also indicates clouds in the northeast and northern parts of the domain that are absent in the MM5 predictions. However, as indicated in Figure 1, the broadband transmissivity for most of the observed clouds for this day is high, meaning that most of the clouds are not thick and will not affect the photolysis rates significantly. But the area around Galveston Bay, including Houston, is covered with thick clouds that are missing in the MM5 predictions. This is significant, as this area is the major source of emissions for ozone precursors.

An error in the prediction of thick clouds over the emissions sources has major consequences. Thick clouds (as seen in Figure 1) can significantly alter the cloud transmissivity and thus the photolysis rates. Over the source regions, an alteration (reduction in this case) in the photolysis rate has both a direct and an indirect impact on ozone chemistry. First, by slowing down the photochemistry, lower photolysis rates inhibit ozone production in the immediate vicinity of emissions sources (direct impact). Second, due to the suppression of photochemistry, lifetime of ozone precursors is increased and the precursors can be transported to the regions where the air mass has a different chemical composition (indirect impact). In the case of Galveston Bay region, since NOx and VOCs are co-emitted, the inhibition of the photochemistry directly impacts the rapid formation of ozone in this area. By doing so, both NOx and VOC remain active for a longer period of time and are transported out of the area. In short, such an event alters the chemical aging of the air mass, and the air mass continues to have the potential of producing ozone for a longer period of time during transport.

Another indirect impact of this scenario is the alteration in partitioning of nitrogen oxides and the impact on nitrate budget due to surface deposition losses. In the presence of thick clouds over the emissions sources of NOx, nitrogen monoxide rapidly consumes ozone and produces nitrogen dioxide. Therefore, while the partitioning of NOx between NO and NO2 has been altered, there is a net increase in NOx. Due to the slow down in the photochemistry, most of the NOx will remain intact and will not be lost in the ozone production to produce nitrates. The major loss for NOx in this situation is the surface removal, and the rate of surface removal for NOx is an order of magnitude less than that of nitric acid (HNO3) [Biazar, 1995]. Therefore, in the absence of clouds over the Galveston Bay area in the control case, there is a much larger loss of total nitrogen oxides (NOy) due to surface removal. Examining a grid point close to the bay (southeast of Houston at 29.7N, 95.3W) reveals that the absence of clouds increased the surface removal of HNO3 for several hours for up to 9 ppb. The loss positively correlates with the increased ozone production and is the result of increased HNO3 production due to active photochemistry. The inclusion of clouds resulted in less than 1 ppb loss of NOx in this case.

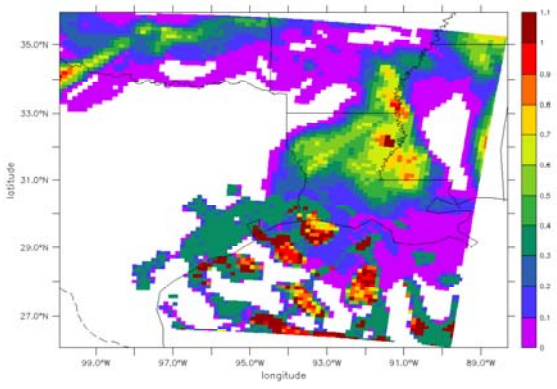

Figure 3. MM5 predicted cloud fraction for August 28, 19 GMT.

In contrast to the August 24 case, on August 28, MM5 predicts a large area of cloudiness over western Mississippi, southern Arkansas, and Louisiana extending to the south Texas (Figure 3). This is absent in the GOES observation. GOES observations indicate subgrid cloudiness to the western part of Texas. The observed clouds are highly transparent and do not alter the photolysis rates significantly. Therefore in this case we have a significant ozone formation in the vicinity of the emission sources that would be absent in the control simulation.

The impact of such alterations in the photolysis rates on the local atmospheric chemical composition can be substantial, especially on the chemical species with the shorter photochemical lifetime. Figure 4 exhibits the largest differences

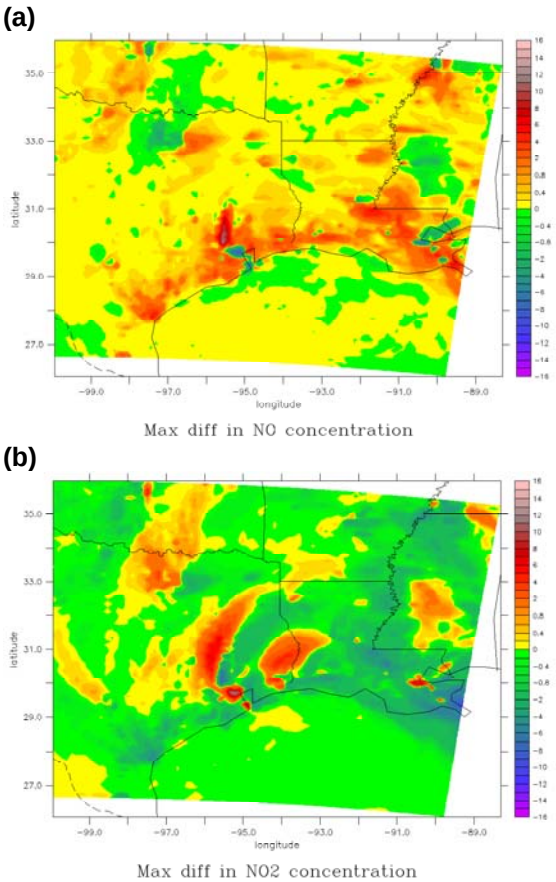

Figure 4. Extreme differences in **a)** NO, and **b)** NO2 between assimilation and control simulations (assim-control) for the entire period of study covering from 0 GMT, August 24, 2000, to 0 GMT, September 1, 2000.

in NO and NO2 between the assimilation and control simulations over the entire period of study. The figure represents the extreme cases of discrepancy between control and assimilation simulations, and these extremes may not occur at the same time. However, the larger values probably represent the same time period, as the negative/positive values for NO are co-located with the positive/negative values of NO2. The areas marked with a large negative NO difference between the assimilation and control correspond to the situation where MM5 predicts cloud, where

in fact there is no cloud in the observation and therefore most of NO is converted to NO2 (and vise versa). These areas are confined to the large source regions as evident for example over the Houston-Galveston Bay area indicating a much faster photochemical activity and rapid ozone formation.

For the NO2 case (Figure 4b) there are broader areas of large discrepancy. Over the Texas region, this indicates the transport of NOx outside the source region where the lifetime of NO2 is increased. This is perhaps due to the transport and dilution of the air mass outside the source region and mixing with an air mass of lower VOC where the rapid ozone formation is inhibited. The evidence for the above statement can be seen in Figure 5 in which the extreme ozone differences are depicted.

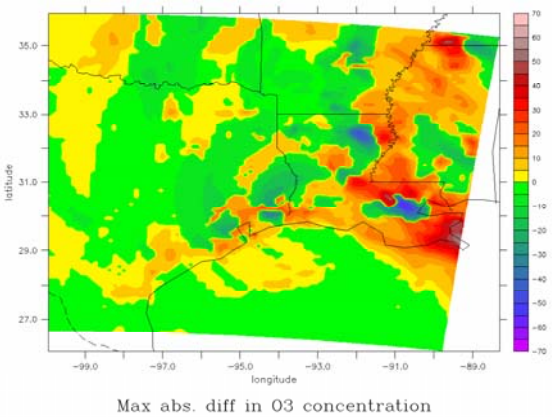

Figure 5. Extreme differences in a) NOx, and b) O3 between assimilation and control simulations (assim-control) for the entire period of study covering from 0 GMT, August 24, 2000, to 0 GMT, September 1, 2000.

Figure 5 also indicates that there are times that the impact of our method on ozone concentration can be quite high (as much as 60 ppb). While these extreme cases are mostly localized in space and time, sustained differences of several ppb over broader areas are more common. Comparing the extreme values of NOx and ozone, there is a good correlation between higher ozone concentrations in the assimilation run and lower NOx concentrations (and lower NO2 concentrations). This indicates the presence of observed clear sky in contrast to MM5 over-predictions of clouds. Therefore the assimilation run produces more ozone and nitrates at the expense of NOx. On the other hand, under-predictions of clouds in MM5 resulted in higher ozone values in the control run for the east/southeast and northern part of Louisiana and a large part of central Texas.

It should be noted, however, that the domain averaged differences only show a maximum of 2 ppb for August 26 and are mostly between +/- 1 ppb. They also exhibit a diurnal variation with higher predicted ozone for the assimilation run.

6. Summary

In this study we used satellite retrieved cloud transmissivity, cloud top height, and observed cloud fraction to correct photolysis rates for cloud cover in CMAQ. We performed CMAQ simulations using this method and compared the results with a simulation that used standard MM5 predictions as input. The simulations were performed at 4- and 12-km resolution domains over Texas, extending east to Mississippi, for the period of August 24 to August 31, 2000.

The results clearly indicate that not using the cloud observations in the model can drastically alter the predicted atmospheric chemical composition within the boundary layer and exaggerate or under-predict ozone concentration. Cloud impact is acute and more pronounced over the emission source regions and can lead to drastic errors in the model predictions of ozone and its precursors. Clouds also increased the lifetime of ozone precursors leading to their transport out of the source regions and causing further ozone production down wind. Longer lifetime for NOx and its transport over regions high in biogenic hydrocarbon emissions (in the eastern part of the domain) led to increased ozone production that was missing in the control simulation.

It should be noted that the modeling domain was extremely dry during the time period of this study. Therefore, the impact of inclusion of observed clouds on photochemistry during other periods with more cloud formation could be even more drastic than what was presented in this study. Such drastic errors can constitute major problems in the use of photochemical models for case studies as well as air quality forecasting. In case studies, simply an inconsistency between the observed cloud field and that of the model can result in erroneous concentrations. Such model predictions then cannot be used to explain the in-situ measurements. Air quality forecast models often use the model results from the previous forecast (or some adjusted form of it) to initialize

the model for the new forecast. Therefore, the errors arising from an inconsistency in the cloud fields can propagate into the future forecasts.

Acknowledgments. This work was accomplished under partial support from Texas Commission on Environmental Quality (TCEQ) and the following grants: U.S. EPA Star Grant R-826770-01-0, Southern Oxidant Study, U.S. EPA Cooperative Agreement R-82897701-0 and Texas Air Research Center/Lamar University contracts TARC/LU-052UAL0030A and 123UAL2030A. Note the results in this study do not necessarily reflect policy or science positions by the funding agencies.

References

Allen, C. W., 1963: *Astrophysical quantities*. Athlene Press, 291 pp.

Allen, David, Cyril Durrenberger, and TNRCC Technical Analysis Division, 2002: Accelerated Science Evaluation of Ozone formation in the Houston-Galveston Area: Photochemical air quality modeling, Technical Report, Texas Commission on Environmental Management, February 2002, 47 pp. http://www.utexas.edu/research/ceer/texaqsarchive/pdfs/Modeling02_17_02.PDF

Barker, H. W., Stephens, G. L., Partain, P. T., Bergman, J. W., Bonnel, B., Campana, K., Clothiaux, E. E., Clough, S., Cusack, S., Delamere, J., Edwards, J., Evans, K. F., Fouquart, Y., Freidenreich, S., Galin, V., Hou, Y., Kato, S., Li, J., Mlawer, E., Morcrette, J.-J., O'Hirok, W., Räisänen, P., Ramaswamy, V., Ritter, B., Rozanov, E., Schlesinger, M., Shibata, K., Sporyshev, P., Sun, Z., Wendisch, M., Wood, N., Yang, F. 2003: Assessing 1D Atmospheric Solar Radiative Transfer Models: Interpretation and Handling of Unresolved Clouds. *Journal of Climate*, **Vol. 16**, No. 16, pp. 2676–2699.

Biazar, A. P., The role of natural nitrogen oxides in ozone production in the Southeastern environment, *Ph. D. Dissertation*, Atmospheric Science Department, University of Alabama in Huntsville, 271 pp., 1995.

Castro, T., Ruiz-Su!arez, L.G., Ruiz-Su!arez, J.C., Molina, M.J., Montero, M., 1997. Sensitivityanaly sis of a UV radiation transfer model and experimental photolysis rates of NO2 in the atmosphere of Mexico city. *Atmospheric Environment*, **31**, 609–620.

Chang, J.S., R.A. Brost, I.S.A. Isaksen, S. Madronich, P. Middleton, W.R. Stockwell, and C.J. Walcek, 1987: A three-dimensional eulerian acid deposition model: physical concepts and formulation, *J. Geophys. Res.,* **92 (D12)**: 14681-14700.

Collins, D.R.; Jonsson, H.H.; Liao, H.; Flagan, R.C.; Seinfeld, J.H.; Noone, K.J.; Hering, S.V., 2000. Airborne analysis of the Los Angeles aerosol, *Atmospheric Environment*, **34**, No. 24, pp. 4155-4173

Coulson, K. L., 1959: Characteristics of the radiation emerging from the top of a Rayleigh atmosphere, 1 and 2. *Planet. Space Sci*., **1**, 256-284.

Diak, G. and M. Whipple, 1995: Note on estimating surface sensible heat fluxes using surface temperatures measured from geostationary satellite. J. Geophys. Res., **100**, 25453-25461

Diak, G. R., C. Gautier, 1983: Improvements to a simple physical model for estimating insolation from GOES data. *J. Appl. Meteor*., **22,** 505-508.

Dickerson, R. R., S. Kondragunta, G. Stenchikov, K. L. Civerolo, B. G. Doddridge, B. N. Holben, 1997. The Impact of Aerosols on Solar Ultraviolet Radiation and Photochemical Smog. *Science*, **278**, 827-830.

EPA, 1999: Science Algorithms of the EPA Models-3 Community Multiscale Air Quality (CMAQ) Modeling System. EPA-600/R-99/030.

Fritz, S., and J. S. Winston, 1962: Synoptic use of radiation measurements from satellite TIROS-II. *Mon Weather Review*., **90**, 1-9.

Gautier, C., G. R. Diak, and S. Mass, 1980: A simple physical model for estimating incident solar radiation at the surface from GOES satellite data. *J. Appl. Meteor.* , **19**, 1005-1012.

Grell, G. A., J. Dudhia, and D. R. Stauffer, 1994: *A Description of the Fifth-Generation Penn State/NCAR Mesoscale Model (MM5).* NCAR Technical Note NCAR/TN-398+STR, National Center for Atmospheric Research, Boulder, Colorado.

Grell, G.A., J. Dudhia and D.R. Stauffer, 1994: The Penn State/NCAR Mesoscale Model (MM5). NCAR Technical Note, NCAR/TN-398+STR, 138 pp.

Haines, S. L., R. J. Suggs, and G. J. Jedlovec, 2004: The GOES Product Generation System, NASA Technical Memorandum, NASA/Marshall Space Flight Center (in press).

Jacobson, M. Z., Studying the effects of aerosols on vertical photolysis rate coefficient and temperature profiles over an urban airshed, J. Geophys. Res., 103(D9), 10593-10604, 10.1029/98JD00287, 1998.

Jedlovec, G. J., 1987: Determination of atmospheric moisture structure from high resolution MAMS radiance data. Ph.D. dissertation, University of Wisconsin-Madison, 187 pp. [Available from University Microfilms International, 300 North Zeeb Road, Ann Arbor, MI 48106-2346.]

Jedlovec, G. J., and K. B. Laws, 2001: Operational cloud detection in GOES imagery. Preprints, *11th Conf. on Satellite Meteorology and Oceanography,* Madison, WI, Amer. Meteor. Soc., 412-415.

Jedlovec, G.J., J. A. Lerner, and R. J. Atkinson, 2000: A satellite-derived upper-tropospheric water vapor transport index for climate studies. *J. Appl. Meteor*. **39**, 15-41.

Lacis, A. A., and J. E. Hansen, 1974: A parameterization for absorption of solar radiation in the earth's atmosphere*. J. Atmos. Sci.*, **31**, 118-133.

Liao, H., Y. L. Yung, J. H. Seinfeld, Effects of aerosols on tropospheric photolysis rates in clear and cloudy atmospheres, *J. Geophys. Res.*, **104**(D19), 23697-23708, 10.1029/1999JD900409, 1999.

Madronich, S., 1987: Photodissociation in the atmosphere, 1, actinic flux and the effects of ground reflections and clouds. Journal of Geophysical Research, 92, 9740-9752.

McNider, R. T., and Fred J. Kopp: Specification of the scale and magnitude of thermals used to initiate convection in cloud models. *J. Applied Meteorology*, **Vol. 29**, No.1, January 1990

McNider, R. T., J. A. Song, and S. Q. Kidder, 1995: Assimilation of GOES-derived solar insolation into a mesoscale model for studies of cloud shading effects. *Int. J. Remote Sens., **16***, 2207-2231.

McNider, R.T., A.J. Song, D.M. Casey, P.J. Wetzel, W.L. Crosson, and R.M. Rabin, 1994: Toward a dynamic-t thermodynamic assimilation of satellite surface temperature in numerical atmospheric models. *Mon. Wea. Rev.,* **122,** 2784-2803.

McNider, R.T., W.B. Norris, D. Casey, J.E. Pleim, S. Rosell, W. Lapenta, 1998: Assimilation of satellite data in regional scale models. Pps 25-35. *Air Pollution Modeling and its Application. Plenum Press, New York.*

McNider, R.T., W.B. Norris, D.M. Casey, J.E. Pleim, S.J. Roselle, W.M. Lapenta, 1998: Assimilation of satellite data in regional air quality models, *Air Pollution Modeling and Its Application* XII, S.E. Gryning and N. Chaumerliac (eds.), NATO/CCMS, Plenum Press, NY.

NCAR (2003): MM5 Modeling System Version 3, NCAR website --- http://www.mmm.ucar.edu/mm5/doc1.html.

Paltridge, G. W., 1973: Direct measurement of water vapor absorption of solar radiation in the free atmosphere*. J. Atmos. Sci*., **30**, 156-160.

Ruggaber, A., Dlugi, R., Nakajima, T., 1994. Modelling radiation quantities and photolysis frequencies in the troposphere. *Journal of Atmospheric Chemistry,* **18** , 171–210.

Stephens, G.L., 1978: Radiation Profiles in Extended Water Clouds. II: Parameterization Schemes. *Journal of the Atmospheric Sciences*, Vol. **35**, No. 11, pp. 2123–2132.

Suggs, R.J., G.J. Jedlovec, and A.R. Guillory, 1998: Retrieval of geophysical parameters from GOES: Evaluation of a split window technique. *J. Appl. Meteor.* **37**, 1205-1227.

Suggs, R.J., G.J. Jedlovec, W.M. Lapenta, and S. Haines, 2000: Evaluation of Skin Temperatures Retrieved from GOES-8. *10th Conference on Satellite Meteorology and Oceanography,* AMS, Long Beach, 137-140.

Vuilleumier, Laurent, Jeffrey T. Bamer, Robert A. Harley and Nancy J. Brown, 2001. Evaluation of nitrogen dioxide photolysis rates in an urban area using data from the 1997 Southern California Ozone Study, *Journal of Atmospheric Environment*, **35**, No. 36, pp. 6525-6537.

Gery, M. W., G .Z. Whitten, J. P. Killus, and M. C. Dodge, A photochemical kinetics mechanism for urban and regional scale computer modeling. *J. Geophys. Res.,* **94(D10),** 12,925–12,956, 1989.